

DSCC2020- 24447

## ON THE ZEROS OF AN UNDAMPED THREE-DOF FLEXIBLE SYSTEM

**Siddharth Rath<sup>†</sup>, Leqing Cui, and Shorya Awtar**  
 Precision Systems Design Lab, Mechanical Engineering  
 University of Michigan, Ann Arbor, MI 48103, USA

## ABSTRACT

This paper presents an investigation of zeros in the SISO dynamics of an undamped three-DoF LTI flexible system. Of particular interest are non-minimum phase zeros, which severely impact closed-loop performance. This study uses modal decomposition and zero loci to reveal all types of zeros – marginal minimum phase (MMP), real minimum phase (RMP), real non-minimum phase (RNMP), complex minimum phase (CMP) and complex non-minimum phase (CNMP) – that can exist in the system under various parametric conditions. It is shown that if CNMP zeros occur in the dynamics of an undamped LTI flexible system, they will always occur in a quartet of CMP-CNMP zeros. And, that the simplest undamped LTI flexible system that can exhibit CNMP zeros in its dynamics is a three-DoF system. Motivated by practical examples of flexible systems that exhibit CNMP zeros, the undamped three-DoF system considered in this paper comprises of one rigid-body mode and two flexible modes. For this system, the following conclusions are mathematically established: (1) This system exhibits all possible types of zeros. (2) The precise conditions on modal frequencies and modal residues associated with every possible zero provide a mathematical formulation of the necessary and sufficient conditions for the existence of each type of zero. (3) Alternating signs of modal residues is a necessary condition for the presence of CNMP zeros in the dynamics of this system. Conversely, avoiding alternating signs of modal residues is a sufficient condition to guarantee the absence of CNMP zeros in this system.

## 1. INTRODUCTION AND MOTIVATION

The dynamics of flexible systems is of interest in a wide range of motion and vibration control applications including space structures [1-3], dexterous manipulation [4-8], locomotion [9-10], hard-disk drives [11-13], and flexure mechanisms [14-16], among others. These applications typically require a combination of range, speed, settling time,

noise and disturbance rejection, control robustness, motion accuracy, etc. – performance specifications that are met by careful choice of sensors, actuators, and associated electronics, as well as design of various control strategies [17-19]. Yet, the presence of resonant peaks along with ill-behaved zero dynamics, such as non-minimum phase behavior [20-24], severely limits the performance that can be achieved through the feedback and feedforward control strategies [25-28].

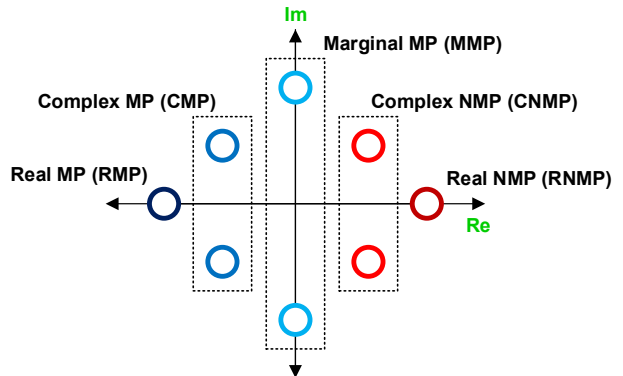


Fig.1 Types of zeros in an LTI system

Fig.1 shows the various types of zeros that can appear in the SISO dynamics of an LTI system – marginal minimum phase (MMP) that lie on the imaginary axis, real minimum phase (RMP), real non-minimum phase (RNMP), complex minimum phase (CMP) and complex non-minimum phase (CNMP). These zeros are dictated by the physical design of the LTI system, including the location of sensor and actuator, and cannot be altered by output or state feedback. Given the critical role that zeros play (particularly NMP zeros) in control performance, an intimate knowledge of the existence of the various types of zeros and their dependence on the various system parameters is of interest.

Section 2 of this paper provides a review of the extensive literature on system zeros. But the existing results fail to present an analysis of systems that include all possible types of zeros. Furthermore, an interpretation of the genesis of zeros

<sup>†</sup>Corresponding Author ([rathsid@umich.edu](mailto:rathsid@umich.edu))

(particularly CNMP zeros) based on physical parameters and design is still lacking. In our previous work, we mathematically predicted [21] and experimentally demonstrated [22] the existence of CNMP zeros under certain combinations of physical parameters and operating conditions in flexure mechanisms. However, this was a system specific investigation, and did not provide a more fundamental understanding into the origin of these zeros.

To achieve such an understanding, we employ modal decomposition [29] to study zeros in the SISO dynamics of an undamped three-DoF LTI flexible system in this paper. This undamped three-DoF flexible system comprises of one rigid-body mode and two flexible modes. The genesis of different types of zeros and their transition from one type to another is shown to depend on precise mathematical conditions that involve the modal frequencies and residues of the flexible system. Since these modal parameters (i.e. frequencies and residues) can be expressed in terms of physical parameters of the system (e.g. stiffness and mass), the mathematical framework presented here offers a direct connection between the zeros and the physical parameters of the system. Therefore, the mathematical framework and associated results of this paper can be used to derive key physical insights into the zero dynamics of any flexible system that can be approximated by the undamped three-DoF LTI flexible system investigated here.

## 2. LITERATURE REVIEW

There is a significant body of research literature on the zero dynamics of flexible systems. Existing frequency domain studies may be broadly classified into three groups: (1) studies that focus on fundamental system types irrespective of the type of zeros, (2) studies that focus on gaining physical meaning into various types of zeros, and (3) studies that focus on specific types of zeros (e.g. CNMP) irrespective of the system type.

Studying the zeros of LTI systems using fundamental system types is based on the idea of modal decomposition [29]. Since a single mode cannot lead to any zeros, the simplest flexible system type to study zeros is a system with two modes or DoF. A simpler variation of this two-DoF system is one where the first mode has zero natural frequency (i.e. is a rigid-body mode). In the literature, Miu [30] used such a two-DoF model for a torsional system and studied the variation of zeros due to the variation of sensor location. Rankers [31] studied the interaction between the rigid body mode and the flexible mode on a frequency response plot. It was demonstrated that the variation of zeros arises due to the variation of modal residues (magnitude and signs) associated with these two modes. Colingh [32] studied a motion stage with flexible guidance and showed the mapping between sensor/actuator locations and various types of zeros. Using a two-DoF flexible system model, this work demonstrated marginally minimum phase (MMP), real minimum phase (RMP) zeros, and real non-minimum phase (RNMP) zeros, but did not capture complex non-minimum phase (CNMP) zeros.

Studying the zeros of systems with a single flexible beam has also been an active area of research. Spector and Flashner [33-34] studied a non-collocated pinned-free beam model and identified the migration of zeros on the real and imaginary axes due to variation in the sensor location. Wie and Bryson [35] studied the pole-zero patterns in flexible structures including beams, membranes and triangular trusses. Lee and Speyer [36] used a Bernoulli-Euler beam model and studied the migration of zeros in various input-output transfer functions. In addition, Aphale [37] studied the zeros of a cantilever beam with the impact of a feed-through term, and Vakil [38] studied the location of zeros for a single flexible beam under the variation of different physical parameters. In all this work, the migration of zeros is restricted to the real and imaginary axes, i.e. zeros are MMP, RMP, or RNMP, but not CMP or CNMP.

There are also studies that focus on zeros of systems that extend beyond a two-DoF model. Tohyama and Lyon [39-40] used a system with two modes and a constant remainder to study the transfer function in room acoustics. By varying the remainder, they identified marginally minimum phase (MMP) zeros and complex non-minimum phase (CNMP) zeros. These studies, however, only provide the variation of the remainder without investigating the influence of changing the two modal residues or frequencies. As a result, RMP and RNMP zeros are not captured in this work. Duffour and Woodhouse [41] studied the transfer function of linearized systems with frictional contact. In their investigation, analytical and graphical locus techniques were used to examine cases with only two modes, with two modes with a constant remainder, and with three modes. While MMP zeros and CNMP zeros are reported in this work, RNMP zeros were not captured due to inadequate spanning of the parameter space. Martin [24] proposed modal decomposition to identify MMP, RNMP, RMP and CNMP zeros by studying a numerical model with three modes, but he did not draw any broader conclusions from his numerical results. He concluded that for the situation of sensor and actuator collocation, the zeros are MMP, wherein zeros are alternately located between the system poles. He also argued that such a system is robust against modelling uncertainties and un-modeled high frequency dynamics when operated in closed loop.

The second group of studies on zeros focus on gaining physical meaning into various types of zeros. Miu [42] studied the MMP zeros in serially connected spring mass systems. He concluded that for this simple class of systems, the MMP zeros indicate the natural frequencies of several sub-systems defined by the actuator and sensor locations. Chandrasekar [43] showed that all the zeros in such serially connected spring-mass systems are MMP zeros. Straete [44] used the approach of bond graphs to study all types of zeros and reached the physical insight that zeros are related to subsystems where energy is “trapped”. In addition, Calafiori’s [45] analysis also characterized how sub-systems are related to zeros. Nevertheless, in all of this work, a sub-system based physical insight is applicable only in simple class of systems, namely

serially connected spring-mass systems. For a general flexible system, sub-systems and any associated physical insights are difficult to identify. Examples include Coelingh's model [32] and the multi-axis flexure mechanism [21-22] that exhibits dynamic coupling between the modes in different axes.

The third group of studies focus on specific types of zeros irrespective of the system type. In particular, CNMP zeros have been reported in flexible systems [21-23], [46-48] but there remains very little physical understanding of these zeros. Cannon and Schmitz [23] identified RNMP and CNMP zeros numerically in the transfer function of a pinned-free beam. Loix et al. [48] studied a four-DoF spring-mass model with spring stiffness variation. They numerically identified the existence of CNMP zeros and the corresponding zero locus. They also provided an experimental observation of CNMP zeros in a cantilever beam set-up but did not present a mathematical formulation for these zeros. Hoagg [49] investigated a three DoF spring-mass-damper model that also captured CNMP zeros. However, they assumed an unusually large damping ratio ( $\zeta > 1.3$ ) to create the CNMP zeros. Awtar [47] predicted and experimentally measured CNMP zeros in the non-collocated transfer function of a multiple spring-mass servo system. Electromagnetic modeling showed that these zeros arise due to a coupling between the DC motor and tachometer in this servo system. In our recent work, CNMP zeros have been modeled [21] and measured [22] in a lightly damped flexure mechanism based motion stage.

In all these studies, the advantage of focusing on specific systems is that it allows one to validate the existence of certain types of zeros (particularly RNMP and CNMP) via models and experiments. Furthermore, the relationship between physical parameters and the location/existence of zeros can be demonstrated. Yet, all these existing studies are system-specific and do not provide a deeper understanding into the existence of zeros for flexible systems in general.

Thus, the gap in the existing literature on zeros may be summarized via two key points. First, while zeros of flexible systems have been studied using the technique of modal decomposition by varying modal parameters, the existing results are incomplete in terms of capturing all possible types of zeros in a single, general flexible system. Second, there remains a lack of physical understanding of the conditions for which certain zeros (especially RNMP and CNMP) appear or change from one type to another.

This paper addresses this gap by identifying the simplest LTI system – an undamped three-DoF flexible system – that exhibits all types of zeros. A mathematical framework based on modal decomposition is used to relate system zeros to modal parameters. Specifically, for a three-DoF flexible system with one rigid-body mode, the precise conditions on modal parameters (frequencies and residues) are derived for every possible zero type. This leads to a comprehensive set of necessary and sufficient conditions on modal parameters for the existence of each type of zero. Since modal parameters can be ultimately correlated to physical parameters of the system (e.g.

stiffness and mass), the mathematical framework presented here can be used to not only gain physical insights into the origin of zero dynamics but also influence them through appropriate choice of physical parameters.

The rest of this paper is organized as follows. *Section 3* captures zero dynamics via modal decomposition and presents key results that help narrow down the scope of this investigation to a three-DoF system. *Section 4* provides an explicit mathematical and graphical correlation between the modal frequencies and residues of a three-DoF flexible system (with one rigid-body mode) and associated zeros. This leads to several important mathematical observations and physical insights. *Section 5* concludes the paper with a summary of the conclusions and design insights obtained in this work and a brief discussion on the future course of this research.

### 3. ZERO DYNAMICS AND MODAL DECOMPOSITION

The input-output dynamics of an LTI SISO system given by transfer function  $G(s)$  can be expressed as the sum of the contributions of its decomposed modes.

$$G(s) = \frac{b_m s^m + \dots + b_1 s + b_0}{a_n s^n + \dots + a_1 s + a_0} = \sum_{i=1}^n \frac{\alpha_i}{s + p_i} \quad (1)$$

**Assumption 1:** The LTI SISO flexible system investigated in this paper is assumed such that all the decomposed modes are second order, and that there are no first order modes. Additionally, it is assumed that these second order modes are all oscillatory in nature, i.e. the poles associated with each mode lie on the imaginary axis and not on the real axis. This is a reasonable assumption for many continuous structural and discrete spring-mass systems.

**Assumption 2:** Next it is assumed that the flexible system is undamped. This assumption is reasonable for flexible systems such as flexure mechanisms that are monolithic with no rolling or sliding joints [14-16], for space structures [1-3], and for machines that operate in vacuum [50], where damping is negligible.

**Assumption 3:** If force is assumed to be the input and displacement is selected as the output of such an LTI SISO flexible system, then the input-output transfer function  $G(s)$  from Eq.(1) can be restated as follows:

$$G(s) = \frac{N(s)}{D(s)} = \frac{b_m s^{2m} + \dots + b_1 s^2 + b_0}{a_n s^{2n} + \dots + a_1 s^2 + a_0} = \sum_{i=1}^n \frac{\alpha_i}{s^2 + \omega_i^2} \quad (2)$$

Here the total number of second order modes is  $n$ , which is also the DoF of the system per the nomenclature of this paper, and  $\omega_i$  is the natural frequency of the  $i^{th}$  mode. Additionally, it is assumed that  $G(s)$  represents a physical system (as opposed to a mathematical system), and is strictly proper, i.e.  $m < n$ . In other words, the number of zero pairs are less than the number of modes in the system.

From Eq. (2), it may be seen that the variation of modal residues ( $\alpha_i$ ) leads to the variation of the numerator coefficients ( $b_i$ ), and thus, the variation of the zeros of  $G(s)$ . There are some

key results that can be readily derived for an LTI SISO flexible system defined by the above assumptions.

**Result 1:** For an undamped LTI flexible system whose SISO dynamics is given by Eq.(2), if a pair of complex non-minimum phase (CNMP) zeros occurs, it will always occur in a quartet along with a pair of complex minimum phase (CMP) zeros.

**Proof:** Transfer function  $G(s)$  can be expressed in terms of its numerator  $N(s)$  and denominator  $D(s)$ , as follows:

$$G(s) = \sum_{i=1}^n \frac{\alpha_i}{s^2 + \omega_i^2} = \frac{\sum_{i=1}^n \left[ \alpha_i \prod_{j \neq i} (s^2 + \omega_j^2) \right]}{\prod_i (s^2 + \omega_i^2)} = \frac{N(s)}{D(s)} \quad (3)$$

As a consequence of the assumptions made above, it is evident that  $N(s)$  and  $D(s)$  are even functions, i.e.,  $N(s) = N(-s)$  and  $D(s) = D(-s)$ .

Therefore, if  $a \pm ib$  (where  $a > 0$ ) are CNMP zeros of  $G(s)$ , i.e.  $N(a \pm ib) = 0$ , and  $N(a \pm ib) = N(-a \pm ib)$  because  $N(s)$  is an even function, then it follows that  $N(-a \pm ib) = 0$ . In other words,  $-a \pm ib$  are also zeros of the  $G(s)$ . Since  $a > 0$  these two zeros constitute a CMP zero pair. Thus, zeros that are neither on the imaginary axis nor on the real axes of the s-plane, always appear as a CMP-CNMP quartet ( $\pm a \pm ib$ ).

**Result 2:** An undamped LTI flexible system has to have a minimum of three modes (i.e. three DoF) to exhibit a CMP-CNMP zero quartet in its SISO dynamics.

**Proof:** According to Result 1, CMP-CNMP zeros always appear as a quartet. This means that for such a quartet to appear, the numerator  $N(s)$  in Eq.(3) should be at least a 4<sup>th</sup> order polynomial in  $s$ . Further, because the physical system is strictly proper, the denominator  $D(s)$  should at least be a 6<sup>th</sup> order polynomial in  $s$ . Since all the decomposed modes of  $G(s)$  are second order, it follows that the system should consist of at least three such modes to exhibit a CMP-CNMP zero quartet.

Based on these results, since a three-DoF undamped LTI flexible system is the simplest system that exhibits CMP-CNMP zeros, we choose this system for the intended investigation that captures all zero types. As discussed in the Literature Review in Section 2, two-DoF undamped LTI flexible systems have been extensively studied [30-32] but exhibit only MMP, RMP and RNMP zeros.

#### 4. THREE-DOF FLEXIBLE LTI SYSTEM

A three-DoF undamped LTI flexible system that follows Assumptions 1 through 3 can be expressed as:

$$G(s) = \frac{\alpha_R}{s^2 + \omega_R^2} + \frac{\alpha_u}{s^2 + \omega_u^2} + \frac{\alpha_v}{s^2 + \omega_v^2} \quad (4)$$

where  $\omega_R < \omega_u < \omega_v$ . Here we make one more assumption – that the first mode is much lower in frequency compared to the subsequent two modes. While a general three-DoF system can be considered, this assumption offers some practical advantages. In previous modeling [21] and experimental [22]

work, we have shown that CNMP zeros appear in systems that have a low-frequency mode and at least two higher frequency closely-spaced modes. This provides the motivation to investigate a slightly simpler system by setting  $\omega_R$  to zero in Eq.(4). This additional assumption also helps simplify the mathematical and graphical analysis of the zero locus in the section, which allows for better physical interpretation of the results.

Yet, the three-DoF model that stems from this assumption can still be used to explain the dynamics of flexible systems that are characterized by a low frequency rigid body mode and a couple of relatively high frequency flexible modes. In such instances, the low-frequency flexible mode is approximated as a pure rigid body mode to study its interaction with the two higher frequency modes, that give rise to the CMP-CNMP zero quartet trapped between them.

Assuming the first mode to be a rigid-body mode, the three-DoF flexible system of Eq.(4) reduces to:

$$G(s) = \frac{\alpha_R}{s^2} + \frac{\alpha_u}{s^2 + \omega_u^2} + \frac{\alpha_v}{s^2 + \omega_v^2} \quad (5)$$

Furthermore,  $\alpha_R$  can be set to be +1, without any loss in generality. This helps reduce the number of parameters that need to be carried through the subsequent mathematical steps. The system transfer function from Eq.(5) maybe further expressed as:  $G(s) =$

$$\frac{\alpha_v s^2 \left[ (1 + \alpha_u / \alpha_v) s^2 + (\alpha_u \omega_v^2 / \alpha_v + \omega_u^2) \right] + [(s^2 + \omega_u^2)(s^2 + \omega_v^2)]}{s^2 (s^2 + \omega_u^2)(s^2 + \omega_v^2)}$$

Next, if we define:

$$\kappa \triangleq \frac{\alpha_u}{\alpha_v} \text{ and } \eta \triangleq \frac{\omega_u^2}{\omega_v^2}$$

then  $G(s)$  may be expressed as:

$$G(s) = \frac{N(s)}{D(s)} = \frac{\alpha_v A(s) + B(s)}{D(s)} \quad (6)$$

where

$$A(s) \triangleq (1 + \kappa) s^4 + \omega_v^2 (\kappa + \eta^2) s^2$$

$$B(s) \triangleq (s^2 + \omega_u^2)(s^2 + \omega_v^2)$$

Now, we create a transfer function  $T(s) = A(s)/B(s)$ , which has no physical meaning and simply serves as a mathematical tool, as described next. First, the poles of  $T(s)$  are the poles associated with modes  $u$  and  $v$ . Second,  $T(s)$  has two pairs of zeros. One pair is fixed at the origin and the other pair changes position based purely on the ratio  $\alpha_u / \alpha_v$ . For a given  $\alpha_u / \alpha_v$  ratio,  $\omega_u$ , and  $\omega_v$ , if  $\alpha_v$  is varied, then the root locus of  $T(s)$  with unity feedback is obtained. But note that the root-locus of  $T(s)$  is also the zero-locus of  $G(s)$ . Moreover, if the sign of  $\alpha_v$  is flipped, then the complementary root locus is obtained. Thus,  $T(s)$  serves as an intermediate mathematical tool to obtain the zero-locus of  $G(s)$  for various modal parameters.

The root-loci of  $T(s)$ , which correspond to the full zero-loci of  $G(s)$ , are shown in Fig.2 for four different value ranges

of  $\alpha_u / \alpha_v$ . For ease of illustration, only the first quadrant is shown in each case. As noted above, the value ranges of  $\alpha_u / \alpha_v$  determine the location range of the second zero pair of  $T(s)$  (shown in blue) as follows:

- (a)  $\frac{\alpha_u}{\alpha_v} > 0$ : 2<sup>nd</sup> zero pair of  $T(s)$  lies between  $\omega_u$  and  $\omega_v$
- (b)  $-\frac{\omega_u^2}{\omega_v^2} < \frac{\alpha_u}{\alpha_v} < 0$ : 2<sup>nd</sup> zero pair of  $T(s)$  lies b/w origin and  $\omega_u$
- (c)  $-1 < \frac{\alpha_u}{\alpha_v} < -\frac{\omega_u^2}{\omega_v^2}$ : 2<sup>nd</sup> zero pair of  $T(s)$  lies on the real axis
- (d)  $\frac{\alpha_u}{\alpha_v} < -1$ : 2<sup>nd</sup> zero pair of  $T(s)$  lies between  $\omega_v$  and infinity

The top panel of Fig.2 shows the zero-loci of  $G(s)$  for positive  $\alpha_v$  (varying from 0 to  $\infty$ ), and the bottom panel shows the zero-loci of  $G(s)$  for negative  $\alpha_v$  (varying from  $-\infty$  to 0). A key observation here is that CNMP zeros arise in instances (b), (c), and (d) of the top panel, where the zero-locus branches break-away from the imaginary axis and subsequently re-join at the real or imaginary axes, as  $\alpha_v$  increases. To find the  $\alpha_v$  value at these break-away and re-join points, one simply needs to find the repeated roots of  $s^2$  in  $N(s)$ , where

$$N(s) = \alpha_v A(s) + B(s)$$

$$= \{1 + \alpha_v(1 + \kappa)\}s^4 + \{\alpha_v(\kappa + \eta^2) + (1 + \eta^2)\}\omega_v^2 s^2 + \omega_u^2 \omega_v^2$$

To find the repeated roots, one can set the discriminant of the above quadratic expression in  $s^2$  to 0,

$$[\{\alpha_v(\kappa + \eta^2) + (1 + \eta^2)\}\omega_v^2]^2 - 4(\omega_u^2 \omega_v^2)\{1 + \alpha_v(1 + \kappa)\} = 0$$

$$\Rightarrow \alpha_v = \frac{-(\kappa - \eta^2)(1 - \eta^2) \pm \sqrt{(1 - \eta^2)|\sqrt{-4\kappa\eta^2}}}{(\kappa + \eta^2)^2}$$

Here, the smaller value of  $\alpha_v$  corresponds to the break-away point and the larger value corresponds to the re-join point:

$$\text{Break-away: } \Rightarrow \alpha_v = \frac{-(\kappa - \eta^2)(1 - \eta^2) - \sqrt{(1 - \eta^2)|\sqrt{-4\kappa\eta^2}}}{(\kappa + \eta^2)^2} \quad (7)$$

$$\text{Re-join: } \Rightarrow \alpha_v = \frac{-(\kappa - \eta^2)(1 - \eta^2) + \sqrt{(1 - \eta^2)|\sqrt{-4\kappa\eta^2}}}{(\kappa + \eta^2)^2}$$

Another key observation in Fig.2 is that a pair of MMP zeros can approach infinity and then transition over to a RMP-RNMP pair, as seen in instance (d) of the top panel and instances (a), (b), and (c) of the bottom panel. The value of  $\alpha_v$  for which this transition happens can be determined by finding the condition when  $N(s)$  has only one pair of roots.

$$N(s) = \alpha_v A(s) + B(s)$$

$$= \{1 + \alpha_v(1 + \kappa)\}s^4 + \{\alpha_v(\kappa + \eta^2) + (1 + \eta^2)\}\omega_v^2 s^2 + \omega_u^2 \omega_v^2$$

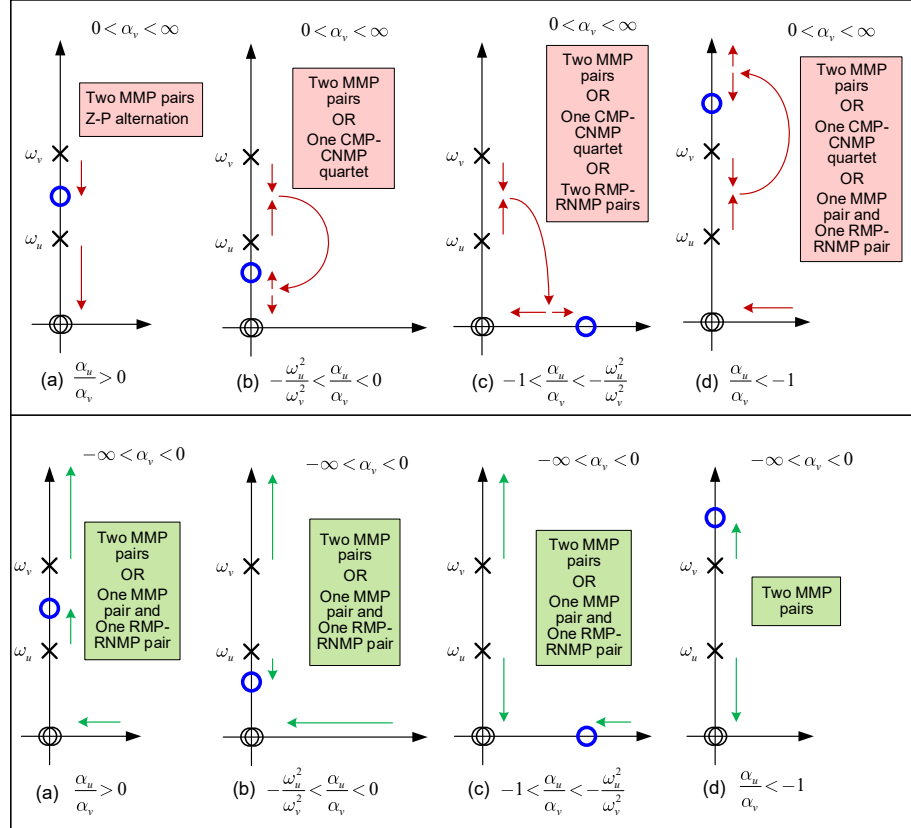


Fig.2. Zero loci of  $G(s)$

This condition corresponds to setting the coefficient of  $s^4$  in the above expression to zero.

$$\{1 + \alpha_v(1 + \kappa)\} = 0 \quad (8)$$

$$\Rightarrow \alpha_v = -\frac{1}{1 + \kappa}$$

Based on these results and Fig.2, the following conclusions can be drawn:

1. By varying  $\alpha_u / \alpha_v$  and  $\alpha_v$ , all types of zeros (i.e. MMP, RMP-RNMP pair and CMP-CNMP quartet) are obtained in the zero loci of a three-DoF flexible system (with one rigid-body mode).
2. CNMP zeros occur in cases (b), (c) and (d) of the top panel where  $(\alpha_u / \alpha_v) < 0$  and  $0 < \alpha_v < \infty$ . Therefore, the necessary condition for the existence of CNMP zeros is the alternating sequence of modal residue signs i.e.  $\alpha_R > 0$  (already assumed to be +1),  $\alpha_u < 0$  and  $\alpha_v > 0$ . This necessary condition is nevertheless not a sufficient condition. As seen in cases (b), (c) and (d) of the top panel, even when the necessary conditions are satisfied, there exist values of  $\alpha_v$  for which the zeros are either MMP or RMP-RNMP. These are the values of  $\alpha_v$  before the break-away and after the re-join of the zero loci, given by Eq.(7).
3. Conversely, avoiding the alternating sequence of modal residue sign is a sufficient condition for the elimination of CNMP zeros. However, this is not a necessary condition for the elimination of CNMP zeros. The value of  $\alpha_v$  can be tuned such that it does not lie between the break-away and re-join points given by Eq.(7). This would guarantee that CNMP zeros do not occur in the system dynamics even in the presence of alternating modal residue signs.
4. Eq.(7) gives the break-away point of the zero loci from the imaginary axis and the subsequent re-join of the zero loci onto the imaginary axis or the real axis. This equation mathematically shows the precise conditions under which MMP zeros transition to CMP-CNMP quartet and then back to either MMP zeros or RMP-RNMP pair. These break-away and re-join points can be easily visualized in instances (b), (c) and (d) of the top panel (i.e.  $0 < \alpha_v < \infty$ ) of Fig.2.
5. Based on Eq.(7), it can be mathematically observed that as  $\eta$  ( $\triangleq \omega_u^2 / \omega_v^2$ ) tends to 1, the values of  $\alpha_v$  at which break-away and re-join occur tend to zero. Therefore, in the presence of alternating sequence of modal residue signs (represented by (b), (c) and (d) when  $0 < \alpha_v < \infty$ ), if a three-DoF flexible system has two closely spaced flexible modes (given by  $\eta$  tending to 1), then the occurrence of CNMP zeros (in form of quartet) becomes very sensitive to small values of  $\alpha_v$ . In the presence of closely spaced flexible modes, even a small non-zero value of  $\alpha_v$  (modal residue associated with the flexible mode  $v$ ), can lead to the presence of CNMP zeros in the system dynamics.
6. Eq.(8) gives the mathematical condition when MMP zeros transition into RMP-RNMP pair. This point of transition only depends on the ratio of modal residues ( $\kappa$ ) of the two flexible modes. If  $\kappa$  tends to -1, then the transition from MMP zeros

to RMP-RNMP pair happens for very large values of  $\alpha_v$ . In other words, the transition becomes insensitive to the value of  $\alpha_v$ .

7. There are two cases, namely case (a) of the top panel and case (d) of the bottom panel where NMP zeros do not occur in the zero locus for any value of  $\alpha_v$ . Case (a) of the top panel leads to a configuration of modal residue signs given by  $\alpha_R > 0$ ,  $\alpha_u > 0$  and  $\alpha_v > 0$ . This is in agreement with [24] where it was shown that when all modal residues have the same sign, it only leads to MMP zeros in the system dynamics.

## 5. CONCLUSION AND FUTURE WORK

This paper investigates the zero dynamics of an undamped 3 DoF flexible system that consists of one rigid body mode and two flexible modes. Precise mathematical conditions are used to provide the necessary and sufficient conditions for the existence of every type of zero (MMP, RMP-RNMP pair and CMP-CNMP quartet) in the system. Particular emphasis is given to NMP zeros, which severely impact the closed loop performance of flexible systems. Based on this investigation, it is found that whenever CNMP zeros occur in the system dynamics, they always occur in a quartet of CMP-CNMP zeros and alternating signs of modal residues are a necessary condition for their occurrence. Therefore, in order to avoid CNMP zeros in the system dynamics, avoiding alternating sequence of modal residue signs is a sufficient condition. The signs of modal residues are closely tied to the location of actuators and sensors on a flexible system through the mode shapes of the associated flexible modes [24]. The mathematical insight from this investigation can be combined with the knowledge of mode shapes of specific flexible systems that can be approximated by an undamped three-DoF flexible system model. This will enable optimal placement of actuators and sensors in order to avoid NMP zeros.

This investigation also reveals that the occurrence of CNMP zeros in undamped three-DoF flexible systems with closely spaced flexible modes is very sensitive to variations in the modal residues and by extension very sensitive to variations in physical parameters of the flexible system [21]. This phenomenon is usually observed in the dynamics of flexure mechanisms that make use of symmetric/periodic building blocks (or flexure modules) to achieve large range of motion, high constraint direction stiffness and low sensitivity to thermal effects [51]. The symmetric/periodic structure gives rise to closely spaced flexible modes and large range of motion gives rise to geometric non-linearities which lead to varying system parameters [21-22].

In this paper, we only presented the investigation on the zeros of an undamped flexible system. In the future, we will also investigate the zero dynamics of damped flexible systems and draw key physical insights on the impact of damping on zero dynamics. We will use these insights to choose actuator-sensor location and damping strategies to show how NMP zeros can be eliminated from the dynamics of large-range multi-axis flexure mechanisms.

## REFERENCES

- [1] S. Di Gennaro, "Output stabilization of flexible spacecraft with active vibration suppression," in *IEEE Transactions on Aerospace and Electronic Systems*, vol. 39, no. 3, pp. 747-759, July 2003.
- [2] Q. Hu, "Sliding mode maneuvering control and active vibration damping of three-axis stabilized flexible spacecraft with actuator dynamics." *Nonlinear Dyn* **52**, 227–248 (2008)
- [3] P. C. Hughes, "Dynamics of flexible space vehicles with active attitude control." *Celestial Mechanics* **9**, 21–39 (1974)
- [4] S. K. Dwivedy and P. Eberhard, "Dynamic analysis of flexible manipulators, a literature review," *Mechanism and Machine Theory*, vol. 41, pp. 749-777, 2006.
- [5] G. Zhu, S. S. Ge, and T. H. Lee, "Simulation studies of tip tracking control of a single-link flexible robot based on a lumped model," *Robotica*, vol. 17, pp. 71-78, Jan-Feb 1999.
- [6] R. Lozano and B. Brogliato, "Adaptive-Control of Robot Manipulators with Flexible Joints," *IEEE Transactions on Automatic Control*, vol. 37, pp. 174-181, Feb 1992.
- [7] M. De Queiroz, S. Donepudi, T. Burg, and D. Dawson, "Model-based control of rigid-link flexible-joint robots: an experimental evaluation," *Robotica*, vol. 16, pp. 11-21, 1998.
- [8] S. M. Megahed and K. Hamza, "Modeling and simulation of planar flexible link manipulators with rigid tip connections to revolute joints," *Robotica*, vol. 22, pp. 285-300, 2004.
- [9] P. Valdivia Y Alvarado, S. Chin, W. Larson, A. Mazumdar, and K. Youcef-Toumi, "A soft body underactuated approach to multi degree of freedom biomimetic robots: A stingray example," *2010 3rd IEEE RAS EMBS Int. Conf. Biomed. Robot. Biomechatronics, BioRob 2010*, pp. 473–478, 2010.
- [10] P. Valdivia y Alvarado and K. Youcef-Toumi, "Design of Machines With Compliant Bodies for Biomimetic Locomotion in Liquid Environments," *J. Dyn. Syst. Meas. Control*, vol. 128, no. 1, p. 3, 2006.
- [11] J. Chang, "Hard disk drive seek-arrival vibration reduction with parametric damped flexible printed circuits." *Microsyst Technol* **13**, 1103–1106 (2007)
- [12] C. La-orpacharapan and L. Y. Pao, "Fast seek control for flexible disk drive systems with back EMF and inductance," *Proceedings of the 2003 American Control Conference, 2003.*, Denver, CO, USA, 2003, pp. 3077-3082 vol.4.
- [13] Feng Gao, Fook Fah Yap and Ying Yan, "Modeling of hard disk drives for vibration analysis using a flexible multibody dynamics formulation," in *IEEE Transactions on Magnetics*, vol. 41, no. 2, pp. 744-749, Feb. 2005.
- [14] K. B. Choi and J. J. Lee, "Passive compliant wafer stage for single-step nano-imprint lithography," *Rev. Sci. Instrum.*, vol. 76, no. 7, 2005.
- [15] N. Roy, A. Yuksel and M. Cullinan, "Design and modeling of a microscale selective laser sintering system," in *11th Int. Manufacturing Science and Engineering Conf.*, V003T08A002 –V003T08A002 (2016).
- [16] M. L. Culpepper and G. Anderson, "Design of a low-cost nano-manipulator which utilizes a monolithic, spatial compliant mechanism," *Precis. Eng.*, vol. 28, no. 4, pp. 469–482, 2004.
- [17] C. Lee and S. M. Salapaka, "Robust broadband nanopositioning: Fundamental trade-offs, analysis, and design in a two-degree-of-freedom control framework," *Nanotechnology*, vol. 20, no. 3, 2009.
- [18] C. Lee and S. M. Salapaka. "Optimal-Control Methods for Design of Two-Degree-Freedom Systems for Nanopositioning." *Proceedings of the ASME 2009 Dynamic Systems and Control Conference. ASME 2009 Dynamic Systems and Control Conference, Volume 2*. Hollywood, California, USA. October 12–14, 2009.
- [19] B. J. Kenton and K. K. Leang, "Design and control of a three-axis serial-kinematic high-bandwidth nanopositioner," *IEEE/ASME Trans. Mechatronics*, vol. 17, no. 2, pp. 356–369, 2012.
- [20] S. Devasia, E. Eleftheriou, and S. O. R. Moheimani, "A Survey of Control Issues in Nanopositioning," *IEEE Trans. Control Syst. Technol.*, vol. 15, no. 5, pp. 802–823, Sep. 2007.
- [21] L. Cui, C. Okwudire, and S. Awtar, "Modeling Complex Nonminimum Phase Zeros in Flexure Mechanisms," *J. Dyn. Syst. Meas. Control*, vol. 139, no. 10, p. 101001, 2017.
- [22] L. Cui, and S. Awtar, 2019, "Experimental Validation of Complex Non-Minimum Phase Zeros in a Flexure Mechanism", *Precision Engineering*, 60, pp. 167-177.
- [23] R. H. Cannon and E. Schmitz, "Initial Experiments on the End-Point Control of a Flexible One-Link Robot," *Int. J. Rob. Res.*, vol. 3, no. 3, pp. 62–75, Sep. 1984.
- [24] G. D. Martin , "On the control of flexible mechanical systems". Ph.D. thesis, Stanford University Department of Aeronautics and Astronautics, 1978.
- [25] J. S. Freudenberg and D. P. Looze, "Right Half Plane Poles and Zeros and Design Tradeoffs in Feedback Systems," *IEEE Trans. Automat. Contr.*, vol. 30, no. 6, pp. 555–565, 1985.
- [26] D.E. Davison, P.T. Kabamba, S.M. Meerkov, "Limitations of disturbance rejection in feedback systems with finite bandwidth", *Automatic Control IEEE Transactions*, vol. 44, no. 6, pp. 1132-1144, 1999.
- [27] Jie Chen, Li Qiu, O. Toker, "Limitations on maximal tracking accuracy", *Automatic Control IEEE Transactions* , vol. 45, no. 2, pp. 326-331, 2000.
- [28] V. Marcopoli, J. Freudenberg, R. Middleton, "Nonminimum phase zeros in the general feedback configuration", *American Control Conference* 2002.

Proceedings of the 2002, vol. 2, pp. 1049-1054 vol.2, 2002.

[29] L. Meirovitch, "Analytical methods in Vibration", vol. 19. New York, NY: *The Mcmillan Company*, 1967.

[30] D. K. Miu, "Mechatronics - Electromechanics and Contromechanics," *Springer*, 1993.

[31] A. M. Rankers, "Machine Dynamics in Mechatronic Systems: An Engineering Approach." Ph.D. thesis, Twente University, The Netherlands, 1997.

[32] E. Coelingh, T. J. A. De Vries, and R. Koster, "Assessment of mechatronic system performance at an early design stage," *IEEE/ASME Trans. Mechatronics*, vol. 7, no. 3, pp. 269–279, 2002.

[33] V. A. Spector and H. Flashner, "Sensitivity of Structural Models for Noncollocated Control Systems," *J. Dyn. Syst. Meas. Control*, vol. 111, no. 4, p. 646, 2009.

[34] V. A. Spector and H. Flashner, "Modeling and Design Implications of Noncollocated Control in Flexible Systems," *J. Dyn. Syst. Meas. Control*, vol. 112, no. 2, p. 186, 2008.

[35] B. Wei and A. E. B. Jr, "Modeling and control of flexible space structures," in *3rd Dynamic and control of large flexible spacecraft, Proceedings of the Third Symposium*, 1981.

[36] Y. J. Lee and J. L. Speyer, "Zero locus of a beam with varying sensor and actuator locations," *J. Guid. Control Dyn.*, vol. 16, no. 1, pp. 21–25, 2008.

[37] S. S. Aphale, A. J. Fleming, and S. O. Reza Moheimani, "Integral resonant control of collocated smart structures," *Smart Mater. Struct.*, vol. 16, no. 2, pp. 439–446, 2007.

[38] M. Vakil, R. Fotouhi, and P. N. Nikiforuk, "On the zeros of the transfer function of flexible link manipulators and their non-minimum phase behaviour," *Proc. Inst. Mech. Eng. Part C J. Mech. Eng. Sci.*, vol. 224, no. 10, pp. 2083–2096, 2010.

[39] M. Tohyama and R. H. Lyon, "Zeros of a transfer function in a multi-degree-of-freedom vibrating system," *J. Acoust. Soc. Am.*, vol. 86, no. 5, pp. 1854–1863, 2005.

[40] M. Tohyama, "Room Transfer Function," *Handb. Signal Process. Acoust.*, no. 1, pp. 1381–1402, 2008.

[41] P. Duffour and J. Woodhouse, "Instability of systems with a frictional point contact. Part 1: Basic modelling," *J. Sound Vib.*, vol. 271, no. 1–2, pp. 365–390, 2004.

[42] D. K. Miu, "Physical Interpretation of Transfer Function Zeros for Simple Control Systems With Mechanical Flexibilities," *J. Dyn. Syst. Meas. Control*, vol. 113, no. 3, p. 419, 2008.

[43] J. Chandrasekar, J. B. Hoagg, and D. S. Bernstein, "On the zeros of asymptotically stable serially connected structures," *2004 43rd IEEE Conf. Decis. Control (IEEE Cat. No.04CH37601)*, vol. 3, pp. 2638-2643 Vol.3, 2008.

[44] H. J. Van de Straete, "Physical meaning of zeros and transmission zeros from bond graph models." M.S. Thesis, Massachusetts Institute of Technology, 1995.

[45] G. C. Calafio, "A subsystems characterization of the zero modes for flexible mechanical structure" *Proceedings of the 36th IEEE Conference on Decision and Control*, San Diego, CA, USA, 1997, pp. 1375-1380 vol.2.

[46] D. F. Enns, "Rocket Stabilization as a Structured Singular Value Synthesis Design Example," *IEEE Control Systems*, vol. 11, no. 4. pp. 67–73, 1991.

[47] S. Awtar, and K. C. Craig , "Electromagnetic Coupling in a dc Motor and Tachometer Assembly ." *ASME. J. Dyn. Sys., Meas., Control.* September 2004; 126(3): 684–691

[48] N. Loix, J. Kozanek, and E. Foltete, "On the complex zeros of non-collocated systems," *Journal of Structural Control*, vol. 3, no. 1-2, pp. 79–87, June 1996.

[49] J. B. Hoagg and D. S. Bernstein, "On the zeros, initial undershoot, and relative degree of lumped-mass structures," in *2006 American Control Conference*, 2006, p. 6 pp.

[50] A. Preumont, "Vibration control of active structures: an introduction", vol. 179, *Springer Science & Business Media*, 2011.

[51] S. Awtar, and G. Parmar, "Design of a Large Range XY Nanopositioning System", *ASME Journal of Mechanisms and Robotics*, 5 (2), 021008 (10 pages), 2013.